Rotational Collision Number and Rotationally Inelastic Cross-Section in Monte Carlo Simulations

Hiroaki Matsumoto

Division of Systems Research, Yokohama National University,
79-5 Tokiwadai, Hodogaya, Yokohama 240-8501, Japan

Abstract. The rotational collision number of nitrogen gas is evaluated using a combination of Monte Carlo integration of Wang-Chang-Uhlenbeck (WCU) theory and classical trajectory calculation (CTC) for diatomic molecules. The rotationally inelastic cross section is also estimated from the rotational collision number presented here and combined with the statistical inelastic cross-section (SICS) model. It is then applied to analysis of the normal shock wave structures for nitrogen. Shock wave structures obtained using the present rotationally inelastic cross-section are compared with results of inelastic cross section based on Parker's energy gain function and experimental data. Results show that shock wave structures given by the proposed rotationally inelastic cross section have better agreement with experimental results than those given by Parker's energy gain function.

Keywords: Rotational collision number, Rotationally inelastic cross section, Diatomic molecules, Monte Carlo simulation, Shock wave structure.
PACS: 02.70.Uu, 07.05.Tp, 02.70.Ns

INTRODUCTION

For Monte Carlo simulation [1] of rarefied gas flow, a realistic and effective molecular collision model or an accurate calculation technique for molecular collision is crucial for realistic simulation. For elastic molecular collisions, accurate and realistic calculation techniques based on scattering theory, as well as simple scattering models [2][3][4] based on kinetic theory have been developed and applied to various rarefied gas flow problems. For a rotationally inelastic molecular collision, a simple model is more practical for engineering because inelastic collision phenomena are complicated; enormous calculation time might be required for accurate approaches such as the classical trajectory calculation (CTC) [5] for diatomic molecules. Some attractive models have been developed, including the dynamic molecular collision (DMC) [6] model, the phenomenological model formulated by Borgnakke-Larsen (BL) [7], and the statistical inelastic cross section (SICS) [8] model.

The BL and SICS models require functions for the inelastic collision probability or inelastic collision cross section to express the inelastic collision number of real gases. Parker's energy gain function, which appears in his approximate theory for the rotational collision number (rotational relaxation time)[9], is widely employed in these models for rotationally inelastic collision for diatomic molecules. Parker's energy gain function, however, is derived with the assumption that pre-collision molecules have no internal energy, which is different from realistic phenomena as well as the collision process in the DSMC simulation.

In the present study, the rotational collision number of nitrogen gas was evaluated using Wang-Chang-Uhlenbeck (WCU) theory [10] with a combination of CTC and Monte Carlo integration to estimate the function for the rotationally inelastic collision probability and rotationally inelastic collision cross-section.

ROTATIONAL COLLISION NUMBER OF DIATOMIC MOLECULES

The first approximations for the rotational collision number $[Z_R]_1$ are defined using the Wang-Chang-Uhlenbeck (WCU) theory [10] as

$$[Z_R]_1 = \frac{4p[\tau_R]_1}{\pi[\eta]_1}, \quad p[\tau_R]_1 = \frac{25}{4}[\varpi]_1 , \tag{1}$$

where p is pressure, $[\tau_R]_1$ is the first approximation of rotational relaxation time, $[\eta]_1$, and $[\varpi]_1$ are the first approximations of viscosity and bulk viscosity coefficients of diatomic molecules, which are defined respectively as

$$\frac{1}{[\eta]_1} = \frac{2}{5kT}\left(a'_{11} - \frac{2}{3}a\right), \tag{2}$$

$$[\varpi]_1 = \frac{2}{25}\frac{kT}{a}, \tag{3}$$

$$a = \frac{1}{Q^2}\left(\frac{kT}{\pi m}\right)^{1/2} \int \exp\left(-\gamma^2 - \tilde{E}_{R1} - \tilde{E}_{R2}\right)\Delta\tilde{E}^2 \gamma b db d\varepsilon d\boldsymbol{\Omega} d\boldsymbol{\Omega}_1 d\gamma, \tag{4}$$

$$a'_{11} = \frac{2}{Q^2}\left(\frac{kT}{\pi m}\right)^{1/2} \int \exp\left(-\gamma^2 - \tilde{E}_{R1} - \tilde{E}_{R2}\right)\left(\gamma^4 - 2\gamma^2\gamma'^2\cos^2\chi + \gamma'^4\right)\gamma b db d\varepsilon d\boldsymbol{\Omega} d\boldsymbol{\Omega}_1 d\gamma, \tag{5}$$

$$Q = \int \exp(-\varepsilon)\, d\boldsymbol{\Omega}\,, \quad \gamma^2 = \frac{\mu g^2}{2kT}\,, \quad \tilde{E}_{Ri} = \frac{E_{Ri}}{kT}\ (i = 1, 2), \tag{6}$$

$$\widetilde{\Delta E} = \widetilde{E}'_{R1} + \widetilde{E}'_{R2} - \tilde{E}_{R1} - \tilde{E}_{R2}, \tag{7}$$

where m, n, k, T, μ, g, and E_{Ri} (i = 1, 2) respectively represent the molecular mass, number density, Boltzmann constant, temperature, reduced mass, relative velocity, and the rotational energy of the colliding molecules, and Q is the classical partition function for the internal modes, Ω represents the phase space for the rotational degree of freedom, and the prime (') symbol denotes the post collision state. In this study, the viscosity and bulk viscosity coefficients given by Eqs. 1–4 were calculated using Monte Carlo integration with the classical trajectory calculation (CTC) for diatomic molecules. The motion of the diatomic molecules was handled as a four-body problem with interaction forces between each pair, except for the pairs that constitute each molecule. In this study, particles 1 and 2 constitute one molecule (molecule 1), and particles 3 and 4 constitute the other (molecule 2). The interatomic distance in each molecule was assumed to remain constant. The motion of each particle is therefore described as

$$m_i \frac{d^2\boldsymbol{r}_i}{dt^2} = -\sum_j \nabla_i \phi_{ij} + \sum_j \lambda_j \frac{\partial h_j}{\partial \boldsymbol{r}_i}, \tag{8}$$

where m_i and r_i denote the mass and spatial coordinates of particle i, ϕ_{ij} is the potential between particles i and j, and ∇_i is the differential operator for r_i. The term h_j is a constraint condition on particle i, which for particles i and j is expressed as

$$h_j = (\boldsymbol{r}_i - \boldsymbol{r}_j)^2 - r_e^2 = 0, \tag{9}$$

where r_e is the interatomic distance in a diatomic molecule, and λ_i are Lagrange indeterminate multipliers set to fulfill the constraint condition after the new time step. In this study, the extended Lennard-Jones potential [11] was employed as given by

$$\begin{aligned}\phi(r_{ij}) = {} & 4\varepsilon_{LJ}\left(\frac{r_g}{d_{LJ}}\right)^{-12}\left\{1 + B\left[P_2(\cos\chi_1) + P_2(\cos\chi_1)\right]\right\} \\ & - 4\varepsilon_{LJ}\left(\frac{r_g}{d_{LJ}}\right)^{-6}\left\{1 + A\left[P_2(\cos\chi_1) + P_2(\cos\chi_1)\right]\right\},\end{aligned} \tag{10}$$

$$\boldsymbol{r}_g = (m_3\boldsymbol{r}_3 + m_4\boldsymbol{r}_4)/(m_3 + m_4) - (m_1\boldsymbol{r}_1 + m_2\boldsymbol{r}_2)/(m_1 + m_2), \tag{11}$$

$$\cos\chi_1 = \boldsymbol{r}_g \cdot \boldsymbol{r}_{12} / |\boldsymbol{r}_g| \cdot |\boldsymbol{r}_{12}|, \cos\chi_2 = \boldsymbol{r}_g \cdot \boldsymbol{r}_{34} / |\boldsymbol{r}_g| \cdot |\boldsymbol{r}_{34}|, \tag{12}$$

$$\boldsymbol{r}_{12} = \boldsymbol{r}_1 - \boldsymbol{r}_2\,, \boldsymbol{r}_{34} = \boldsymbol{r}_3 - \boldsymbol{r}_4\,, \tag{13}$$

where P_2 is the second Legendre Polynomial, ε_{LJ} is the potential well, d_{LJ} is the size parameter, and A and B are anisotropy parameters. The interatomic distance, molecular mass, and the parameters of extended Lennard-Jones potential for nitrogen molecules are listed in Table I.

The initial position $\boldsymbol{r}_i$ and velocity vector $\boldsymbol{u}_i$ are applied to each particle. The particle trajectory is calculated using Eq. 8 by the RATTLE method [12]. The initial velocity vectors and positions were determined by the following equations with the initial relative velocity g assigned from the Maxwellian velocity distribution function and the initial rotational energies E_{R1} and E_{R2} assigned from the Boltzmann distribution function for rotational energy.

$$\boldsymbol{r}_1 = -\frac{m_{34}}{M}\frac{\boldsymbol{g}}{|\boldsymbol{g}|}r_0 + \frac{b}{2}\boldsymbol{e}_0 + \frac{m_1}{m_{12}}\frac{r_e}{2}\frac{\boldsymbol{r}_{12}}{|\boldsymbol{r}_{12}|}, \tag{14}$$

$$\boldsymbol{r}_2 = -\frac{m_{34}}{M}\frac{\boldsymbol{g}}{|\boldsymbol{g}|}r_0 + \frac{b}{2}\boldsymbol{e}_0 - \frac{m_1}{m_{12}}\frac{r_e}{2}\frac{\boldsymbol{r}_{12}}{|\boldsymbol{r}_{12}|}, \tag{15}$$

$$\boldsymbol{r}_3 = \frac{m_{12}}{M}\frac{\boldsymbol{g}}{|\boldsymbol{g}|}r_0 - \frac{b}{2}\boldsymbol{e}_0 + \frac{m_3}{m_{34}}\frac{r_e}{2}\frac{\boldsymbol{r}_{34}}{|\boldsymbol{r}_{34}|}, \tag{16}$$

$$\boldsymbol{r}_4 = \frac{m_{12}}{M}\frac{\boldsymbol{g}}{|\boldsymbol{g}|}r_0 - \frac{b}{2}\boldsymbol{e}_0 - \frac{m_4}{m_{34}}\frac{r_e}{2}\frac{\boldsymbol{r}_{34}}{|\boldsymbol{r}_{34}|}, \tag{17}$$

$$\boldsymbol{u}_1 = \frac{m_{34}}{M}\boldsymbol{g} + \sqrt{\frac{m_2}{m_1}\frac{2E_{R12}}{m_{12}}}\boldsymbol{e}_{12} + \sqrt{\frac{m_2}{m_1}\frac{2E'_{R12}}{m_{12}}}\boldsymbol{e}'_{12}, \tag{18}$$

$$\boldsymbol{u}_2 = \frac{m_{34}}{M}\boldsymbol{g} - \sqrt{\frac{m_1}{m_2}\frac{2E_{R12}}{m_{12}}}\boldsymbol{e}_{12} - \sqrt{\frac{m_1}{m_2}\frac{2E'_{R12}}{m_{12}}}\boldsymbol{e}'_{12}, \tag{19}$$

$$\boldsymbol{u}_3 = -\frac{m_{12}}{M}\boldsymbol{g} + \sqrt{\frac{m_4}{m_3}\frac{2E_{R34}}{m_{34}}}\boldsymbol{e}_{34} + \sqrt{\frac{m_4}{m_3}\frac{2E'_{R34}}{m_{34}}}\boldsymbol{e}'_{34}, \tag{20}$$

$$\boldsymbol{u}_4 = -\frac{m_{12}}{M}\boldsymbol{g} - \sqrt{\frac{m_3}{m_4}\frac{2E_{R34}}{m_{34}}}\boldsymbol{e}_{34} + \sqrt{\frac{m_3}{m_4}\frac{2E'_{R34}}{m_{34}}}\boldsymbol{e}'_{34}, \tag{21}$$

$$M = \sum_i m_i, \; m_{ij} = m_i + m_j, \tag{22}$$

$$\boldsymbol{g} = g\boldsymbol{e}_r, \tag{23}$$

$$E_{R12} = E_{R1}R_{nd}, \; E'_{R12} = E_{R1}\left(1 - R_{nd}\right), \tag{24}$$

$$E_{R34} = E_{R2}R_{nd}, \; E'_{R34} = E_{R2}\left(1 - R_{nd}\right). \tag{25}$$

In those equations, R_{nd} is a uniform random number in the range [0,1], and $\boldsymbol{e}_r$ is arbitrary unit vector, $\boldsymbol{e}_0$ expresses a unit vector perpendicular to $\boldsymbol{e}_r$, and r_0 represents the initial separation of centers between colliding molecules, $\boldsymbol{e}_{12}$ and $\boldsymbol{e}_{12}$' are unit vectors perpendicular to $\boldsymbol{r}_{12}$, and $\boldsymbol{e}_{34}$ and $\boldsymbol{e}_{34}$' are unit vectors perpendicular to $\boldsymbol{r}_{34}$. The impact parameter b is determined using the probability density function

$$b = b_{\max}\sqrt{R_{nd}}. \tag{26}$$

Here, $b_{\max}$ is given by the following equation, which is based on the relation between the cutoff angle $\chi_{\min}$ in a monatomic molecule and the maximum impact parameter $(b_{\max})_{el}$ [5]:

$$b_{\max} = \left(b_{\max}\right)_{el} + r_e \tag{27}$$

$$\left(b_{\max}\right)_{el} = \max\left[\left(\frac{32\pi}{\chi_{\min}}\frac{\varepsilon_{LJ}}{\mu g^2}\right)^{1/6}, \left(\frac{64\pi}{\chi_{\min}}\frac{\varepsilon_{LJ}}{\mu g^2}\right)^{1/12}\right]d_{LJ}. \tag{28}$$

The initial separation of centers between colliding molecules (r_0) is then given by the following expression from Ref. [5]:

$$r_0 = \max\left[3\cdot d_{LJ}, 1.1\cdot b_{\max}\right]. \tag{29}$$

Figure 1 shows the comparison of rotational collision number Z_R among the CTC, Parker's approximate theory, and experimental data [13]. The rotational collision number predicted in this study took a large value in the temperature range of $T \leq 500$ K and a small value in the temperature range of $T \geq 500$ K than Parker's approximate

theory, as shown Fig.1, but both Z_R predicted in this study and Parker's approximate theory are in reasonable agreement with the experimental results.

ROTATIONALLY INELASTIC CROSS SECTION OF DIATOMIC MOLECULE

The rotationally inelastic cross section in the SICS model is defined as

$$\sigma_R = \sigma_{el}\zeta\left(E/\varepsilon_0\right), E = E_{tr} + E_{R1} + E_{R2}, \tag{30}$$

where σ_{el} is the elastic collision cross section, ζ is the function for rotational inelastic collision, and ε_0 is the reference energy. Parker's energy gain function ζ_{Parker} is employed widely in SICS and BL models.

In this study the variable soft sphere model for inverse power law potential $\sigma_{el}=C(E_{tr}/k)^{-\omega}$ is applied to elastic collision, where C and ω are VSS model parameter constants and the function ζ is assumed to be of a form that is similar to the Parker's energy gain function

$$\zeta\left(E/\varepsilon_{LJ}\right) = a_0 + \frac{a_1}{\sqrt{E_{LJ}/\varepsilon_{LJ}}} + \frac{a_2}{E_{LJ}/\varepsilon_{LJ}}, \tag{31}$$

where a_i represents fitting parameters that are determined to describe the rotational collision number of CTC results applying least-squares estimation. Figure 2 shows the rotational collision number estimated using Eqs. 30 and 31 for C = 499.5, ω = 0.359, a_0 = 6.06 × 10^{-2}, a_2 = 0.863, and a_2 = 0.444 compared with the CTC results, Parker's approximate theory, and measured data. As shown in Fig.2, the rotational collision number based on Eq.31 is in reasonable agreement with that of CTC results, although it took a small value in the temperature range of $T \leq 1000$ K and a large value in the temperature range of $T \geq 1000$ K than CTC result.

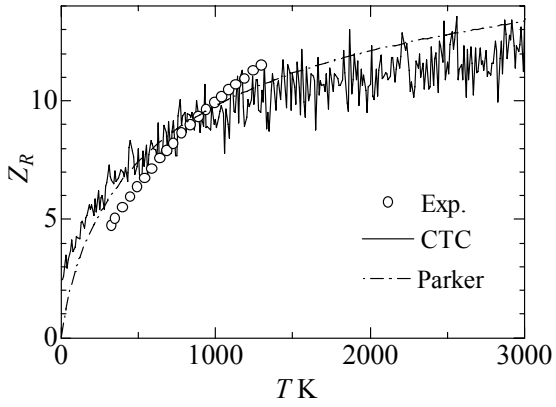

FIGURE 1. Comparison of rotational collision number among the CTC results, Parker's approximate theory, and experimental results.

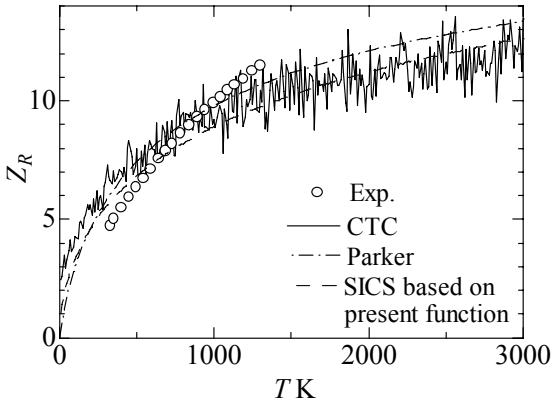

FIGURE 2. Same as Fig. 1 for the present model, CTC results, Parker's approximation theory, and experimental results.

ANALYSIS OF NORMAL SHOCK WAVES STRUCTURE

Calculations were handled as one-dimensional steady-state problems, with flow in the x direction. The flow domain was $-30l_1 \leq x \leq 30l_1$, divided into collision cells and data cells of uniform size $\Delta x = 0.1l_1$, where l_1 is the reference length of the upstream region defined as the following.

$$l_1 = \frac{16}{5}\left(\frac{m}{2\pi kT_1}\right)^{1/2}\frac{\eta_1}{\rho_1} \tag{32}$$

In that equation, η_1 is the viscosity coefficient for monatomic molecules at upstream temperature T_1. The initial wave was placed at the origin ($x = 0$) with a thickness of zero; i.e. the simulation molecules were distributed uniformly in the computation domain according to the upstream ($x < 0$) and downstream ($x > 0$) equilibrium

Maxwellian velocity distributions and equilibrium Boltzmann distributions for rotational energy. The upstream and downstream boundaries were connected to the Rankine-Hugoniot relation. Time was advanced by Δt, each molecule was moved, and molecules that had exited the analysis domain were deleted. Molecules were also introduced via the interfaces in the appropriate equilibrium conditions. Computations for intermolecular collisions occurring in each collision cell during Δt were carried out using the null-collision method [14]. After a steady-state shock wave had formed, the temporal mean of the flow field was taken and the macroscopic physical quantities were calculated. Figures 3 and 4 show distributions of normalized density $n^* = (n - n_1)/(n_2 - n_1)$, normalized translational temperature $T_{tr}^* = (T_{tr} - T_1)/(T_2 - T_1)$, and normalized rotational temperature $T_R^* = (T_R - T_1)/(T_2 - T_1)$ at upstream Mach numbers and temperatures of (M_1, T_1) = (1.71, 191 K), and (12.9, 9.15 K). Subscript "2" in the above definitions refers to the equilibrium condition downstream of the shock wave. The experimental density distribution and rotational temperature distribution [15] are also shown for comparison. The calculation results are shown with a scaled x coordinate to x/L^*, where L^* is the characteristic length used in the experiment, as defined by

$$L^* = \frac{\eta^*}{\rho u}, \quad \rho u = const. \tag{33}$$

Therein, u is the mean velocity in the shock wave, and η^* expresses the viscosity coefficient of N_2 at the speed of sound at sonic temperature T_s and is calculated using Eq. 2. The non-dimensional time step used for the computations was $\Delta(t \times c_m/l_1) = 10^{-4}$, and the number of simulation molecules was set to approximately 100 in each upstream equilibrium cell. Here, c_m is the most probable thermal velocity of the molecules at the upstream temperature. Figures 3 and 4 show that both the model based on ζ and that based on ζ_{Parker} [8] reproduce the experimental density distribution very well at both Mach numbers and that the model based on ζ approaches the experimental rotational temperature distribution more closely than the model based on ζ_{Parker}, although the rotational temperature of ζ relaxed slower than observed in the experiment. Therefore, it appears to be necessary to improve the energy function. Figures 5 and 6 compare the molecular rotational energy distribution within the shock wave obtained using the ζ based model with the experimental results. The figures provide log plots for the ratio of the fraction of molecules in the ground state versus the fraction of molecules in state E_R: $y(E_R)/y(0)$. Lines BD(T_1) and BD(T_2) in the graph respectively represent the upstream and downstream equilibrium Boltzmann distributions. The typical location within the shock wave is where the experimental and calculated values of T_R^* match. Figure 5 shows that the model reproduced the experimental results well at a low Mach number of $M_1 = 1.71$, where $\log[y(E_R)/y(0)]$ is linear, indicating equilibrium. As Fig. 6 also indicates, however, $\log[y(E_R)/y(0)]$ exhibits a bimodal distribution at higher Mach numbers of 12.9, indicating non-equilibrium conditions. This agrees qualitatively with experimental results. However, at $M_1 = 12.9$, the model underestimated the fraction of molecules possessing low rotational energies. Some discrepancies exist in the rotational energy distribution for the highly non-equilibrium state obtained through calculations and experiments, even when the rotational temperatures for the calculation and the experiment are identical. Consequently, the model departs from real phenomena in terms of the exchange between rotational and translational energies during collisions in the highly non-equilibrium region. Therefore, to express microscopic physical quantities such as rotational energy distributions correctly, it appears necessary to make further improvements to the part of the model describing energy distributions in collisions.

CONCLUDING REMARKS

The rotational collision number of a nitrogen molecule was calculated using a combination of classical trajectory calculation of diatomic molecule and Monte Carlo integration of the WCU theory. The rotational collision number predicted in this study is in reasonable agreement with experimental results and the number indicated by estimations using Parker's approximation theory. The rotationally inelastic collision cross section was estimated from the rotational collision number of CTC results. The rotationally inelastic collision cross section obtained by Monte Carlo integration was then incorporated into the SICS model and applied to analysis of the normal shock wave structure. Results show that the proposed model provides results that more closely approximate the experimental results than the model based on Parker's theory. However, predictions of the model in the non-equilibrium region show a delay in the rotational temperature and discrepancies in the rotational energy distribution with respect to experimental results, indicating that the energy gain function and the principles of the energy transfers between translational and rotational energy must be further refined.

TABLE 1. Intearatomic distance, molecular mass and parameters of extended Lennard-Jones potential for nitrogen molecule.

r_e [Å]	m [au]	d_{LJ} [Å]	ε/k [K]	A	B
1.094	28.013	3.681	91.5	0.13	0.7

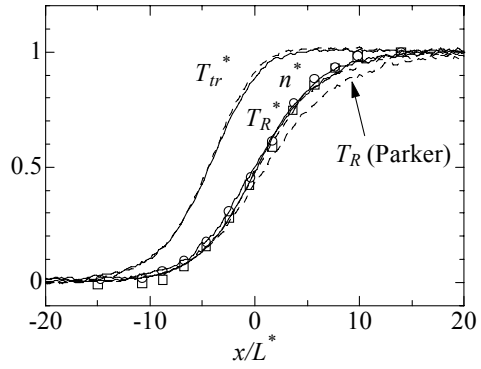

FIGURE 3. Comparison of shock wave structure among the present model, Parker's energy gain function, and experimental data for $M = 1.71$.

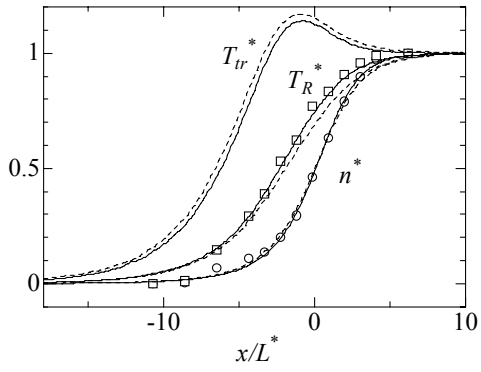

FIGURE 4. Same as Fig.3 for $M = 12.9$

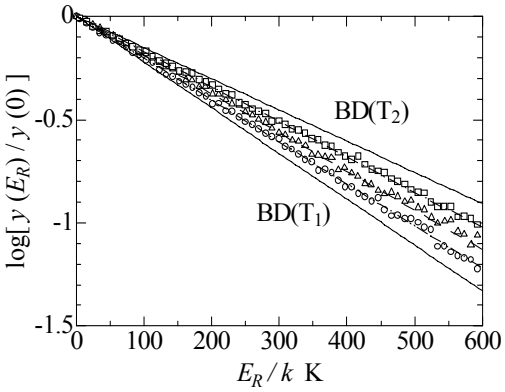

FIGURE 5. Comparison of measured rotational energy distribution (lines) with that determined by SICS with present function (symbols) for a Mach 1.71 nitrogen shock wave. $T^* = 0.079$: $x/L^* = -4.2$ (o), $x/L^* = -6.6$ (— · · —); $T^* = 0.30$: $x/L^* = -1.5$ (Δ), $x/L^* = -2.5$ (- - - -); $T^* = 0.61$: $x/L^* = 2.0$ (□), $x/L^* = 1.7$ (— · — · —).

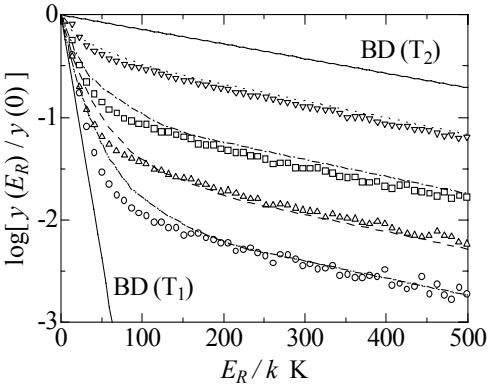

FIGURE 6. Comparison of measured rotational energy distribution (lines) with that determined by SICS with present model for a Mach 12.9 nitrogen shock wave. $T^* = 0.146$: $x/L^* = -6.1$ (○), $x/L^* = -6.5$ (— · · —); $T^* = 0.293$: $x/L^* = -3.1$ (Δ), $x/L^* = -4.4$ (— —); $T^* = 0.532$: $x/L^* = -1.9$ (□), $x/L^* = -2.3$ (— · —); $T^* = 0.769$: $x/L^* = 0.36$ (∇), $x/L^* = -0.13$ (·····).

REFERENCES

1. G. A. Bird, *Molecular Gas Dynamics and the Direct Simulation of Gas Flows*, Clarendon Press (1994).
2. G. A. Bird, *Prog. Astronaut. Aeronaut. AIAA* **74**, 239-255 (1981); G. A. Bird, *Phys. Fluids* **26**, 3222-3223 (1983).
3. K. Koura and H. Matsumoto, *Phys. Fluids* **A3**, 2459-2465 (1991).
4. H. Matsumoto, *Phys. Fluids* **14**, 4256-4265 (2002).
5. K. Koura, K., *Phys. Fluids* **9**, 3543-3549 (1997).
6. T. Tokumasu and Y. Matsumoto, *Phys. Fluids* **11**, 1907-1920 (1999).
7. C. Borgnakke and P. S. Larsen, *J. Comput. Phys*. **18**, 405-420 (1975).
8. K. Koura, *Phys. Fluids* **A4**, 1782-1788 (1992); K. Koura, *Phys. Fluids* **A5**, 778-780 (1993).
9. J. G. Parker, *Phys. Fluids* **2**, 449-462 (1959).
10. S. Chapman and T. G. Cowling, The Mathematical Theory of Non-Uniform Gases, Cambridge Univ. Press, 3rd edition, (1976): 1st edition, (1939).
11. M. D. Pattengill and R. B. Bernstein, *J. Chem. Phys*. **65**, 4007-4015 (1976).
12. J. P. Ryckaert, G. Ciccotti, and H. J. C. Berendsen, *J. Comp. Phys*. **23**, 327-341 (1977).
13. E. H. Carnevale, C. Carey, and G. Larson, *J. Chem. Phys*. **47**, 2829-2835 (1967).
14. K. Koura, *Phys. Fluids*, **29**, 3509-3511 (1986).
15. F. Robben and L. Talbot, *Phys. Fluids*, **9**, 653-662 (1964).